Macro to micro

Microwave remote sensing of plant water content for physiology and ecology

Konings, Alexandra G.; Rao, Krishna; Steele-Dunne, Susan C.

DOI
10.1111/nph.15808

Publication date
2019

Document Version
Final published version

Published in
New Phytologist

Tansley insight

Macro to micro: microwave remote sensing of plant water content for physiology and ecology

Author for correspondence:
Alexandra G. Konings
Tel: +1 650 736 2083
Email: konings@stanford.edu

Received: *28 December 2018*
Accepted: *5 March 2019*

Alexandra G. Konings[1], Krishna Rao[1] and Susan C. Steele-Dunne[2]

[1]Department of Earth System Science, Stanford University, 473 Via Ortega, Room 140, Stanford, CA 94305, USA; [2]Faculty of Civil Engineering and Geosciences, Delft University of Technology (TU Delft), Stevinweg 1, Delft 2628 CN, the Netherlands

Contents

New Phytologist (2019) **223:** 1166–1172
doi: 10.1111/nph.15808

Key words: leaf water potential, microwave remote sensing, plant water content, radar, radiometry, relative water content, vegetation optical depth.

Summary

Although primarily valued for their suitability for oceanographic applications and soil moisture estimation, microwave remote sensing observations are also sensitive to plant water content (M_w). Since M_w depends on both plant water status and biomass, these observations have the potential to be useful for a range of plant drought response studies. In this paper, we introduce the principles behind microwave remote sensing observations to illustrate how they are sensitive to plant water content and discuss the relationship between landscape-scale M_w and common stand-scale metrics, including plant-scale relative water content, live fuel moisture content and leaf water potential. Lastly, we discuss how various sensor types can be leveraged for specific applications depending on the spatio-temporal resolution needed.

I. Introduction

Since the development of plant hydraulic theories (Cowan, 1965), most research concerning the movement of water through vascular plants has been performed at the stand scale or smaller. In recent years, modelling plant hydraulics at larger scales has become increasingly common, whether for predicting drought-driven tree mortality (e.g., Tai *et al.*, 2016), water and carbon fluxes (e.g., Bohrer *et al.*, 2005), or both (Christoffersen *et al.*, 2016). To ensure their accuracy, such models must be carefully parametrized and tested against observations. This has resulted in an increasing need for large-scale observations of plant water status.

In situ measurements of variables relevant to plant hydraulics, including leaf water potential (Ψ_l) and xylem water potential (Ψ_x), remain sparse. Unlike forest inventory networks for biomass or the FluxNet family of networks for eddy-covariance observations (Chu *et al.*, 2017), no standardized network exists for plant hydraulics. Remotely sensed observations that can be used for plant hydraulic (and other) applications would enable a range of new investigations.

Satellite observations at microwave frequencies are directly sensitive to plant water content (M_w), here defined as the total mass of water in the above-ground components of the plant per unit land area. These observations therefore carry information relevant to plant water stress, which could be useful for both plant hydraulic and other studies. In this paper, we provide an overview of the opportunities and pitfalls for using microwave observations for ecological studies. In order to clarify what information can and cannot be gleaned from microwave observations, Section II describes the physical basis behind their sensitivity to M_w.

Section III then clarifies the relationship between M_w and commonly used metrics of plant drought status. Lastly, because several of these relationships remain indirect, Section IV discusses the role of co-sensitivity of microwave remote sensing to biomass and water stress, and how the time and spatial scales of interest determine the best choice of microwave observables.

Note that this paper is focused on microwave-frequency observations. While optical (Zarco-Tejada *et al.*, 2003) and hyperspectral sensors (Kokaly *et al.*, 2009) are also sensitive to canopy water status, the utility of such data for plant hydraulic studies is more limited because they cannot observe through cloud cover, and primarily sense the top of the canopy only.

II. Microwave remote sensing of vegetation

Microwaves are electromagnetic (EM) waves with wavelengths from 1 mm to 1 m, or 0.3–300 GHz in terms of frequency. They fall between the infrared and radiowaves parts of the EM spectrum. Frequency ranges up to *c.* 14 GHz are most useful for sensing M_w. Within this range, longer wavelengths (lower frequencies) can pass further through the canopy and soil, and are more sensitive to soil moisture (Steele-Dunne *et al.*, 2017). Microwave instruments can either be passive (radiometer) or active (radar). The former observe naturally emitted radiation from the land surface, and typically have a coarse resolution (> 10 km). Radars transmit an EM wave and measure the amount of backscatter. Spaceborne real aperture radars (scatterometers) provide resolutions comparable to those from radiometry, while synthetic aperture radars (SAR) can yield dramatically higher resolutions (meter-scale).

Much of our understanding of microwave interactions with vegetation comes from research motivated by soil moisture retrieval in which the vegetation is primarily viewed as a hindrance. Vegetation is analyzed as a collection of constituents (i.e. leaves, trunks, and fruits). Microwave interactions with vegetation are dominated by absorption and scattering (and, for radiometry, emission), both of which depend on the dielectric constant, volume fraction, and arrangement of the vegetation constituents (Ulaby & Jedlicka, 1984; Ulaby *et al.*, 2014). The dielectric constant of a material is a property that determines how it responds to an electric field. For vegetation, it depends primarily on the fractional volume composed of water (El-rayes & Ulaby, 1987). This sensitivity to water is central to the value of microwave remote sensing for ecology.

In radiometry, microwave emission from a vegetated surface is expressed as brightness temperature ($T_{B,p}$) at polarization p, the temperature of an equivalent pure blackbody with the same emitted radiation. It is commonly described by three contributions: soil, vegetation, and their interactions (Fig. 1a):

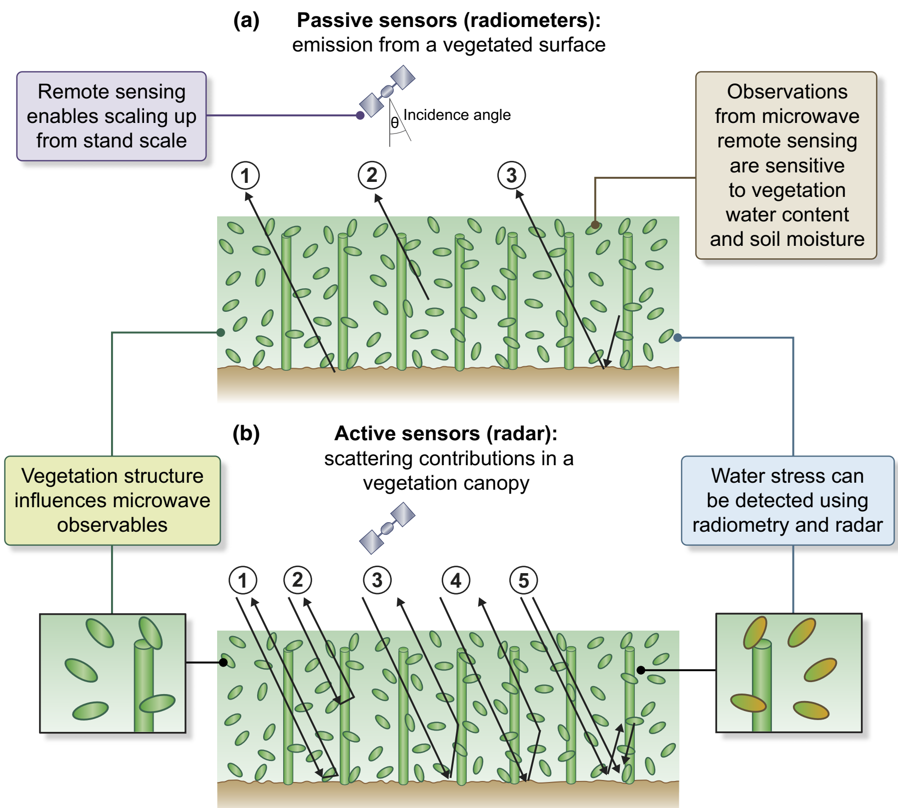

Fig. 1 A cross-section of vegetation illustrating how it is typically treated in microwave remote sensing as a random distribution of idealized vegetation components. Contributions to emission from a vegetated canopy (a) include (1) emission from the soil attenuated by the overlying vegetation, (2) emission from the vegetation itself, (3) emission from the vegetation that is reflected from the soil and attenuated by the vegetation. Scattering contributions from a vegetation canopy (b) include (1) direct backscattering from soil, including two-way attenuation by canopy, (2) direct backscattering from plants, (3) plant/ground scattering, (4) ground/plant scattering, (5) ground/plant/ground scattering (Ulaby *et al.*, 2014).

$$T_{B,p} = e_{s,p} T_s \gamma + (1-\omega)(1-\gamma) T_v + (1-\omega)(1-e_{s,p}) T_v (1-\gamma)\gamma, \quad \text{Eqn 1}$$

where $e_{s,p}$ is the soil emissivity, T_s and T_v are the soil and vegetation temperatures, ω is the single-scattering albedo and γ is the transmissivity. Radiometry has been widely used for soil moisture retrieval due to the sensitivity of $T_{B,p}$ to $e_{s,p}$, which varies with soil moisture (Njoku & Entekhabi, 1996). Most VOD retrieval algorithms use brightness temperatures at two EM wave polarizations to separate soil moisture and vegetation effects. The ω captures how much the EM wave is scattered as it passes through vegetation, relative to how much vegetation attenuates the wave. This is not an ecologically relevant quantity, though it can depend somewhat on vegetation geometry. Many (though not all) retrieval algorithms assume it varies only with land cover type. The T_s and T_v are either obtained from reanalysis or from thermal or high EM-frequency microwave observations. Together with ω, spatial heterogeneity and uncertainty in T_s and T_v are important error sources in radiometric retrieval algorithms (Lei *et al.*, 2015).

Vegetation water dynamics are observable through their influence on the transmissivity γ, which is a measure of how much the vegetation attenuates the signal from the soil surface. Transmissivity (for both active and passive) is given by:

$$\gamma = \exp\left(\frac{-\text{VOD}}{\cos\theta}\right), \quad \text{Eqn 2}$$

where θ is the incidence angle and the vegetation optical depth VOD is widely approximated as a linear function of M_w (Jackson & Schmugge, 1991):

$$\text{VOD} = bM_w \quad \text{Eqn 3}$$

In reality, VOD also depends on structure/geometry and dielectric properties of vegetation (Kirdiashev *et al.*, 1979). This relationship has been verified for a number of vegetation types, though only over crops and grasses (Jackson & Schmugge, 1991). For a given wavelength, b is often assumed static and parametrized as a function of land cover type only. This may induce some error, but the factors affecting b are sufficiently complex and poorly understood to make this an appropriate assumption (Van de Griend & Wigneron, 2004). Note that because b depends on wavelength, values of VOD from different sensors cannot be directly compared.

Alternatively, for radar, backscatter from a vegetation canopy consists of several contributions, illustrated in Fig. 1(b). Their relative dominance depends on system characteristics (e.g., EM frequency, polarization, incidence angle) as well as the vegetation dielectric properties and geometry (Steele-Dunne *et al.*, 2017). The structure of the vegetation plays a larger role in radar than in radiometry, though it is often difficult to parametrize. The most widely used model for scattering from vegetated surfaces is the Water Cloud Model (Attema & Ulaby, 1978), in which the vegetation is characterized as a homogeneous cloud comprised of uniformly distributed water droplets in a layer above the soil surface. The total backscatter (σ°) is expressed as the combination of contributions from the vegetation layer (σ°_{veg}), and the soil (σ°_s):

$$\sigma^\circ = \gamma^2 \sigma^\circ_s + \sigma^\circ_{veg} \quad \text{Eqn 4}$$

$$\sigma^\circ_{veg} = (1-\gamma^2) A\cos\theta, \quad \text{Eqn 5}$$

where γ^2 is the two-way attenuation through the vegetation, and A is a canopy descriptor. The two terms in Eqn 4 correspond to the attenuated backscatter from the soil and direct scattering from vegetation, respectively, denoted by (1) and (2) in Fig. 1(b). Multiple scattering between the soil and canopy, and within the canopy is ignored (3–5 in Fig. 1b). The model assumes that vegetation can be described by its height and the cloud density, which is generally assumed to be proportional to M_w. Recently, this model has been used to produce global estimates of VOD from the Advanced Scatterometer (ASCAT) data (Vreugdenhil *et al.*, 2016). More theoretical models also exist and are useful to demonstrate feasibility or conduct sensitivity studies (e.g., Tsang & Kong, 1981; Ulaby *et al.*, 1990; Bracaglia *et al.*, 1995). However, their widespread use is hindered by the large set of input parameters required to describe canopy properties that are seldom measured by ecologists. Alternatively, many studies using radar for vegetation applications interpret only the raw backscatter instead of trying to isolate the vegetation signal through γ, particularly in densely vegetated regions where the EM waves may not penetrate deeply enough to be sensitive to soil moisture.

Radars and radiometers each have advantages and disadvantages – while radars like SAR have higher spatial resolution, they are sensitive to vegetation structure, whereas radiometers allow easy retrieval of VOD, but are sensitive to temperature and ω. Dew or canopy intercepted water are commonly neglected for either sensor. For a given study, the choice of microwave dataset is influenced not just by sensor type but also by factors like record length, frequency, orbital characteristics, data sharing policy etc.

III. Linking physiological and remote sensing quantities

Since microwave observables (backscatter and VOD) can be related to M_w, we describe the relationship between M_w and various plant-related quantities used in stand-scale studies in this section. Table 1 shows the mathematical relationships between them. Definitions are separated into biomass and water status components, since M_w is related to both. Indeed, both radar (Santoro *et al.*, 2015) and radiometry (Liu *et al.*, 2015; Brandt *et al.*, 2018) have previously been used to estimate wall-to-wall biomass maps, although the sensitivity of microwave measurements to plant water status adds uncertainty to these estimates, as further discussed in Section IV.

For both biomass and live fuel moisture content (LFMC) – a commonly used quantity in fire studies – the relevant definitions are identical across scales. Independent biomass maps can be obtained from Light Detection and Ranging (LiDAR; Zolkos *et al.*, 2013) and ancillary information. Unfortunately, LiDAR measurements

Table 1 Stand-scale metrics used in plant physiology linked to landscape-scale quantities obtainable from microwave observables.

Quantity	Stand scale	Remote sensing scale
Biomass	$AGB = \frac{M_d}{A}$	
Water Status	$RWC = \frac{M_f - M_d}{M_t - M_d}$, $\Psi_x = f(RWC)$	$M_w = \frac{M_f - M_d}{A}$
	$LFMC = \frac{M_f - M_d}{M_d} = \frac{M_w}{AGB}$	

M_f, fresh mass of vegetation; M_d, dry mass of vegetation; M_t, turgid mass of vegetation in its fully hydrated state; RWC, relative water content; Ψ_x, xylem water potential; *f*, non-linear function estimated by fitting parameters (see Fig. 2); *A*, ground-area spanned by vegetation canopy; AGB, above-ground dry biomass per area; M_w, plant water content; LFMC, live fuel moisture content.

are not currently available at the same spatio-temporal coverage as microwave observations, though the recently launched Global Ecosystem Dynamics Investigation (GEDI) sensor (Dubayah *et al.*, 2014) will significantly increase their availability. With independent biomass estimates, ecosystem-scale LFMC can be computed from microwave-derived M_w.

Other water stress metrics are more difficult to scale-up. The relative water content (RWC) – a quantity relevant to drought-driven mortality estimation (Bartlett *et al.*, 2012; Martinez-Vilalta *et al.*, 2018) – is generally defined relative to the mass of water under turgid conditions (M_t). The M_t varies with plant size and species and thus has no obvious equivalent at the landscape-scale for microwave remote sensing. The M_w can be exactly written as:

$$M_w = \mathrm{RWC} \times \frac{M_t - M_d}{A}. \qquad \text{Eqn 6}$$

The second term is difficult to estimate with remote sensing. It is conceptually related to $M_{w,max}$, the maximum observed M_w at a location, but is not exactly the same because M_t and M_d change with time due to phenology and growth. Overall, to transform M_w into a metric related to water *stress* rather than water *status*, some normalization is necessary – this could be either through $M_{w,max}$ or above-ground dry biomass per unit area (AGB) as in the calculation of LFMC.

By far the most common measure of plant water status is the water potential (Ψ) in a plant component – leaves (Ψ_l), xylem (Ψ_x), or elsewhere. It is therefore natural to ask how M_w is related to plant-averaged Ψ. As shown in Fig. 2, many studies have shown a relationship between Ψ_x and RWC, although the exact functional form depends on the study and species. A direct conversion from microwave observables to Ψ thus remains out of reach. Nevertheless, the monotonicity of the curves in Fig. 2 suggests that a local linearization of the M_w-Ψ relationship could be possible. Indeed, when applied to a multi-year time series at a deciduous forest in Missouri, the root-mean-square-error of a linearization was only 5% (see supplementary material in Konings & Gentine, 2017). The relationship between M_w and Ψ_l was also tested by Momen *et al.* (2017), who compared VOD retrieved from the Advanced Microwave Scanning Radiometer AMSR-E to *in situ* measurements of Ψ_l at three forested sites (both mixed and deciduous) across North America. Despite large differences in scale between the satellite footprint (25×25 km^2) and *in situ* measurements at just a few trees, VOD and Ψ_l were moderately well-correlated at all sites, and would be expected to be even more closely related if more careful up-scaling were possible.

Note that the relative contributions of water potential in leaves (Ψ_l) and xylem (Ψ_x) to microwave observables are poorly understood because they depend on species, frequency, and water content (microwaves pass further through canopies with less water and at lower frequencies, see Section II). Despite these complexities, as discussed above, microwave observables do carry information about variations in Ψ_x and Ψ_l.

IV. Approaches for interpreting M_w variations across scales

The co-sensitivity of microwave observables to both AGB and vegetation water status complicates the interpretation of their spatial and temporal trends. Careful consideration of spatial and temporal scales can facilitate the interpretation of microwave observables. Depending on the application area, observations of either high spatial resolution (promoting the use of SAR) or high temporal resolution (often requiring radiometry or scatterometry) may be more useful, leading to a natural choice of sensor for many studies (Fig. 3). For example, wildfires are particularly sensitive to

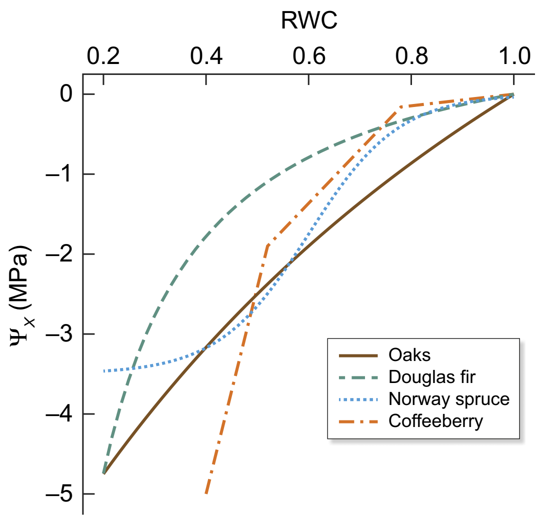

Fig. 2 Comparison of fitted models of relative water content (RWC) and xylem water potential (Ψ_x) found in the literature. The line for oaks was calculated using simulations from the finite difference ecosystem-scale tree crown hydrodynamics model version 2 (FETCH2) by Mirfenderesgi *et al.* (2016), the Douglas fir fit-line was drawn based on Barnard *et al.* (2011), the Norway spruce fit-line was calculated based on Zweifel *et al.* (2000) and the line for Coffeeberry (*Frangula californica*) was constructed using data from Pratt & Jacobsen (2017).

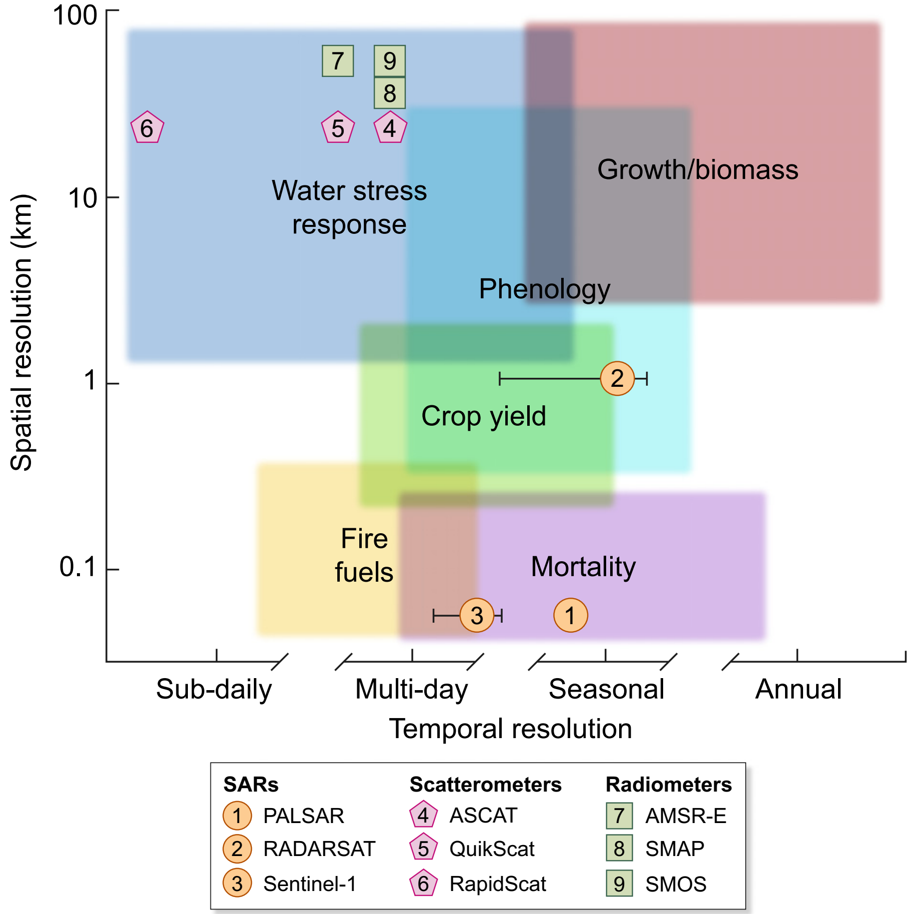

Fig. 3 Temporal and spatial scales relevant to several applications, compared to resolution of representative microwave sensors of different types. A sensor can be used if its spatial and temporal resolutions are within or finer than the resolution scales relevant to a particular application. Horizontal bars around SAR sensors indicate acquisition variability. While the left-most end of error bar indicates how often a given location could theoretically be observed, data rate limitations means observations are only acquired at a subset of the time (often irregular) resulting in a range of revisit frequencies depending on geographic location. Abbreviations are as follows: SAR, synthetic aperture radar; PALSAR, Phased Array type L-band Synthetic Aperture Radar; ASCAT, Advanced Scatterometer; AMSR-E, Advanced Microwave Scanning Radiometer for Earth Observing System; SMAP, Soil Moisture Active Passive; SMOS, Soil Moisture Ocean Salinity.

fine-scale spatial variations in fire fuels, so SAR backscatter may be well-suited for their study (Saatchi *et al.*, 2007). By contrast, studies that aim to validate regional-scale land surface models – which rarely resolve scales below tens of kilometers anyway – could use radiometric VOD and exploit its higher temporal revisit.

Regardless of spatial scale, some timescales are difficult to interpret. For example, variations in M_w in deciduous forests across days-to-weeks are influenced by both phenology (Tian *et al.*, 2017) and changes in RWC. Even if ancillary LAI data are known, disentangling these is mathematically difficult without knowing woody biomass dynamics. However, separation of timescales between growth and water-stress related physiological processes can help. The role of water stress is isolated when considering timescales during which there is little variation in biomass. For example, at daily-scale, biomass variations are negligible. If other contributions can be accounted for (e.g., rain, soil moisture), variations in microwave observables can therefore be interpreted as solely due to water stress (Steele-Dunne *et al.*, 2012). This approach was used to investigate the dynamics of canopy water content in the tropics using the RapidScat radar aboard the International Space Station, whose orbit allows the calculation of an average diurnal cycle (van Emmerik *et al.*, 2017; Konings *et al.*, 2017b). The slope of midnight vs midday observations of VOD has also been used to calculate ecosystem-scale isohydricity using radiometer-derived VOD (Konings & Gentine, 2017), which influences the drought-sensitivity of photosynthesis in North American grasslands (Konings *et al.*, 2017a).

If variations in biomass are assumed small during the peak growing season, this period could also be used to isolate day-to-day variations in plant water status. For example, when Momen *et al.* (2017) compared up-scaled ground-measurements of Ψ_l and VOD at three North American forested sites during the growing season, LAI variations played a relatively minor role – accounting also for LAI instead of Ψ_l only led to only a small increase in the explained VOD variance.

By contrast, no clear approach exists for removing the effect of water stress from VOD. Various studies have used trends in VOD to determine biomass trends (e.g., Liu *et al.*, 2015; Brandt *et al.*, 2018). These studies generally compare a snapshot of VOD to a static map of biomass. Once a regression between VOD and AGB is established across space, trends in VOD are assumed proportional to trends in AGB, thereby implicitly assuming that if average water stress effects on VOD across *space* are small (as indicated by the correlation quality), they must also be small in *time*. However, the resulting global relative trends in biomass are *c.* 0.6% per year or less (Liu *et al.*, 2015), a value smaller than or similar to relative trends in soil moisture (Dorigo *et al.*, 2012) – a possible proxy for M_w. Thus, VOD trends induced by trends in LFMC may add significant uncertainty to biomass trend analyses. Careful comparison of VOD only at periods with similar water stress levels (such as the most saturated conditions) could reduce this uncertainty.

V. Next steps

The strategies detailed above are useful for interpreting microwave observables in the context of specific applications (Section IV). So far, most applications of these observables have focused on simply comparing the data to other remotely sensed variables (e.g., gross primary productivity in Teubner *et al.* 2018 or a variety of canopy size and meteorological indices in others, such as Konings *et al.*, 2017b and Liu *et al.*, 2018). To derive further ecological and plant physiological insights, new frameworks are needed that either explicitly disentangle the quantities in Table 1 from M_w, or new frameworks need to be developed for data assimilation of microwave observables in ecological models. Doing so will also require improved error characterization of the observations. For this purpose, new validation campaigns that explicitly compare microwave observables to physiological metrics (Section III) are sorely needed, especially those that consider scaling challenges.

Acknowledgements

AGK was supported by NASA Terrestrial Ecology award 80NSSC18K0715 through the New Investigator Program. KR was supported by NASA Earth and Space Science Fellowship. SCS-D was supported by Vidi Grant 14126 from the Applied Engineering and Sciences Domain of the Netherlands Organisation for Scientific Research (NWO).

ORCID

Alexandra G. Konings https://orcid.org/0000-0002-2810-1722
Krishna Rao https://orcid.org/0000-0002-8912-0441
Susan C. Steele-Dunne https://orcid.org/0000-0002-8644-3077

References

Attema EPW, Ulaby FT. 1978. Vegetation modeled as a water cloud. *Radio Science* **13**: 357–364.

Barnard DM, Meinzer FC, Lachenbruch B, Mcculloh KA, Johnson DM, Woodruff DR. 2011. Climate-related trends in sapwood biophysical properties in two conifers: avoidance of hydraulic dysfunction through coordinated adjustments in xylem efficiency, safety and capacitance. *Plant, Cell & Environment* **34**: 643–654.

Bartlett MK, Scoffoni C, Sack L. 2012. The determinants of leaf turgor loss point and prediction of drought tolerance of species and biomes: a global meta-analysis. *Ecology Letters* **15**: 393–405.

Bohrer G, Mourad H, Laursen TA, Drewry D, Avissar R, Poggi D, Oren R, Katul GG. 2005. Finite element tree crown hydrodynamics model (FETCH) using porous media flow within branching elements: a new representation of tree hydrodynamics. *Water Resources Research* **41**: W11404. doi: 10.1029/2005WR004181.

Bracaglia M, Ferrazzoli P, Guerriero L. 1995. A fully polarimetric multiple scattering model for crops. *Remote Sensing of Environment* **54**: 170–179.

Brandt M, Wigneron JP, Chave J, Tagesson T, Penuelas J, Ciais P, Rasmussen K, Tian F, Mbow C, Al-Yaari A *et al.* 2018. Satellite passive microwaves reveal recent climate-induced carbon losses in African drylands. *Nature Ecology and Evolution* **2**: 827–835.

Christoffersen BO, Gloor M, Fauset S, Fyllas NM, Galbraith DR, Baker TR, Kruijt B, Rowland L, Fisher RA, Binks OJ *et al.* 2016. Linking hydraulic traits to tropical forest function in a size-structured and trait-driven model (TFS vol 1-Hydro). *Geoscientific Model Development* **9**: 4227–4255.

Chu H, Baldocchi DD, John R, Wolf S, Reichstein M. 2017. Fluxes all of the time? A primer on the temporal representativeness of FLUXNET. *Journal of Geophysical Research: Biogeosciences* **122**: 289–307.

Cowan I. 1965. Transport of water in the soil–plant–atmosphere system. *Journal of Applied Ecology* **2**: 221–239.

Dorigo W, De Jeu R, Chung D, Parinussa R, Liu Y, Wagner W, Fernández-Prieto D. 2012. Evaluating global trends (1988–2010) in harmonized multi-satellite surface soil moisture. *Geophysical Research Letters* **39**: 3–9.

Dubayah R, Goetz SJ, Blair JB, Fatoyinbo TE, Hansen M, Healey SP, Hofton MA, Hurtt GC, Kellner J, Luthcke SB *et al.* 2014. *The global ecosystem dynamics investigation. AGU Fall Meeting Abstracts*, U14A-07.

El-rayes MA, Ulaby FT. 1987. Microwave dielectric spectrum of vegetation-Part I: Experimental observations. *IEEE Transactions on Geoscience and Remote Sensing* **GE 25**: 541–549.

van Emmerik T, Steele-Dunne S, Paget A, Oliveira RS, Bittencourt PR, Barros FdV, van de Giesen N. 2017. Water stress detection in the Amazon using radar. *Geophysical Research Letters* **44**: 6841–6849.

Jackson TJ, Schmugge TJ. 1991. Vegetation effects on the microwave emission of soils. *Remote Sensing of Environment* **36**: 203–212.

Kirdiashev K, Chukhlantsev A, Shutko A. 1979. Microwave radiation of the earth's surface in the presence of vegetation cover. *Radiotekhnika i Elektronika* **24**: 256–264.

Kokaly RF, Asner GP, Ollinger SV, Martin ME, Wessman CA. 2009. Characterizing canopy biochemistry from imaging spectroscopy and its application to ecosystem studies. *Remote Sensing of Environment* **113**(Suppl. 1): S78–S91.

Konings A, Yu Y, Xu L, Yang Y, Schimel D, Saatchi S. 2017b. Active microwave observations of diurnal and seasonal variations of canopy water content across the humid African tropical forests. *Geophysical Research Letters* **44**: 2290–2299.

Konings AG, Gentine P. 2017. Global variations in ecosystem-scale isohydricity. *Global Change Biology* **23**: 891–905.

Konings AG, Williams AP, Gentine P. 2017a. Sensitivity of grassland productivity to aridity controlled by stomatal and xylem regulation. *Nature Geoscience* **10**: 284–288.

Lei F, Crow WT, Shen H, Parinussa RM, Holmes TRH. 2015. The impact of local acquisition time on the accuracy of microwave surface soil moisture retrievals over the contiguous United States. *Remote Sensing* **7**: 13448–13465.

Liu YY, van Dijk AIJM, de Jeu RaM, Canadell JG, McCabe MF, Evans JP, Wang G. 2015. Recent reversal in loss of global terrestrial biomass. *Nature Climate Change* **5**: 470–474.

Liu YY, van Dijk AIJM, Miralles DG, McCabe MF, Evans JP, de Jeu RAM, Gentine P, Huete A, Parinussa R, Wang L *et al.* 2018. Enhanced canopy growth precedes senescence in 2005 and 2010 Amazonian droughts. *Remote Sensing of Environment* **211**: 26–37.

Martinez-Vilalta J, Anderegg WRL, Sapes G, Sala A. 2018. Greater focus on water pools may improve our ability to understand and anticipate drought-induced mortality in plants. *New Phytologist*. doi:10.1111/nph.15644.

Mirfenderesgi G, Bohrer G, Matheny AM, Fatichi S, de Moraes Frasson RP, Schäfer KV. 2016. Tree level hydrodynamic approach for resolving aboveground water storage and stomatal conductance and modeling the effects of tree hydraulic strategy. *Journal of Geophysical Research: Biogeosciences* **121**: 1792–1813.

Momen M, Wood JD, Novick KA, Pangle R, Pockman WT, McDowell NG, Konings AG. 2017. Interacting effects of leaf water potential and biomass on vegetation optical depth. *Journal of Geophysical Research: Biogeosciences* **122**: 3031–3046.

Njoku EG, Entekhabi D. 1996. Passive microwave remote sensing of soil moisture. *Journal of Hydrology* **184**: 101–129.

Pratt RB, Jacobsen AL. 2017. Conflicting demands on angiosperm xylem: tradeoffs among storage, transport and biomechanics. *Plant, Cell & Environment* **40**: 897–913.

Saatchi S, Halligan K, Despain D, Crabtree R. 2007. Estimation of forest fuel load from radar remote sensing. *IEEE Transactions on Geoscience and Remote Sensing* **45**: 1726–1740.

Santoro M, Beaudoin A, Beer C, Cartus O, Fransson JE, Hall RJ, Pathe C, Schmullius C, Schepaschenko D, Shvidenko A *et al.* 2015. Forest growing stock volume of the northern hemisphere: spatially explicit estimates for 2010 derived from Envisat ASAR. *Remote Sensing of Environment* **168**: 316–334.

Steele-Dunne SC, Friesen J, Van De Giesen N. 2012. Using diurnal variation in backscatter to detect vegetation water stress. *IEEE Transactions on Geoscience and Remote Sensing* **50**(7 PART1): 2618–2629.

Steele-Dunne SC, McNairn H, Monsivais-Huertero A, Judge J, Liu P, Papathanassiou K. 2017. Radar remote sensing of agricultural canopies: A review. *IEEE Journal of Selected Topics in Applied Earth Observations and Remote Sensing* **10**: 2249–2273.

Tai X, Mackay DS, Anderegg WRL, Sperry JS, Brooks PD. 2016. Plant hydraulics improves and topography mediates prediction of aspen mortality in southwestern USA. *New Phytologist* **213**: 113–127.

Teubner IE, Forkel M, Jung M, Liu YY, Miralles DG, Parinussa R, van der Schalie R, Vreugdenhil M, Schwalm CR, Tramontana G *et al.* 2018. Assessing the relationship between microwave vegetation optical depth and gross primary production. *International Journal of Applied Earth Observation and Geoinformation* **65**: 79–91.

Tian F, Brandt M, Liu YY, Rasmussen K, Fensholt R. 2017. Mapping gains and losses in woody vegetation across global tropical drylands. *Global Change Biology* **23**: 1748–1760.

Tsang L, Kong JA. 1981. Application of strong fluctuation random medium theory to scattering from vegetation-like half space. *IEEE Transactions on Geoscience and Remote Sensing* **GE-19**: 62–69.

Ulaby FT, Jedlicka RP. 1984. Microwave dielectric properties of plant materials. *IEEE Transactions on Geoscience and Remote Sensing* **GE-22**: 406–415.

Ulaby FT, Long DG, Blackwell WJ, Elachi C, Fung AK, Ruf C, Sarabandi K, Zebker HA, Van Zyl J. 2014. *Microwave radar and radiometric remote sensing*, vol 4. Ann Arbor, MI, USA: University of Michigan Press.

Ulaby FT, Sarabandi K, McDonald K, Whitt M, Dobson MC. 1990. Michigan microwave canopy scattering model. *International Journal of Remote Sensing* **11**: 1223–1253.

Van de Griend A, Wigneron J-P. 2004. On the measurement of microwave vegetation properties: some guidelines for a protocol. *IEEE Transactions on Geoscience and Remote Sensing* **42**: 2277–2289.

Vreugdenhil M, Dorigo WA, Wagner W, Jeu RAMd, Hahn S, Marle MJEv. 2016. Analyzing the vegetation parameterization in the TU-Wien ASCAT soil moisture retrieval. *IEEE Transactions on Geoscience and Remote Sensing* **54**: 3513–3531.

Zarco-Tejada PJ, Rueda CA, Ustin SL. 2003. Water content estimation in vegetation with MODIS reflectance data and model inversion methods. *Remote Sensing of Environment* **85**: 109–124.

Zolkos SG, Goetz SJ, Dubayah R. 2013. A meta-analysis of terrestrial aboveground biomass estimation using lidar remote sensing. *Remote Sensing of Environment* **128**: 289–298.

Zweifel R, Item H, Häsler R. 2000. Stem radius changes and their relation to stored water in stems of young Norway spruce trees. *Trees* **15**: 50–57.